

Online Resource Management in Energy Harvesting BS Sites through Prediction and Soft-Scaling of Computing Resources

Thembelihle Dlamini*[†], Ángel Fernández Gambín*, Daniele Munaretto[†], Michele Rossi*

*Department of Information Engineering, University of Padova, Padova, Italy

[†]Athonet, Bolzano Vicentino, Vicenza, Italy

{dlamini, afgambin, rossi}@dei.unipd.it, daniele.munaretto@athonet.com

Abstract—Multi-Access Edge Computing (MEC) is a paradigm for handling delay sensitive services that require ultra-low latency at the access network. With it, computing and communications are performed within one Base Station (BS) site, where the computation resources are in the form of Virtual Machines (VMs) (computer emulators) in the MEC server. MEC and Energy Harvesting (EH) BSs, i.e., BSs equipped with EH equipments, are foreseen as a key towards next generation mobile networks. In fact, EH systems are expected to decrease the energy drained from the electricity grid and facilitate the deployment of BSs in remote places, extending network coverage and making energy self-sufficiency possible in remote/rural sites. In this paper, we propose an online optimization algorithm called ENergy Aware and Adaptive Management (ENAAM), for managing remote BS sites through foresighted control policies exploiting (short-term) traffic load and harvested energy forecasts. Our numerical results reveal that ENAAM achieves energy savings with respect to the case where no energy management is applied, ranging from 56% to 66% through the scaling of computing resources, and keeps the server utilization factor between 30% and 96% over time (with an average of 75%). Notable benefits are also found against heuristic energy management techniques.

Index Terms—energy harvesting, mobile edge computing, energy self-sustainability, soft-scaling, limited lookahead controller.

I. INTRODUCTION

Multi-Access Edge Computing (MEC) [1] (formerly known as Mobile Edge Computing) has recently emerged as a key solution to process workloads at the network edge, i.e., at the BSs, while passing the less time-constraint workloads to the remote cloud. This network design paradigm is based on Network Function Virtualization (NFV), where mobile network functions (NFs) that formerly existed in the Evolved Packet Core (EPC) are moved to the network edge, such as user's services, which are deployed on local cloud platforms located close to the BSs. In addition, the 5G Mobile Networks (MNs) carbon footprint can be minimized through the use of EH elements by empowering BSs with green energy, thus reducing their dependence on the power grid [2].

The integration of MEC and EH BSs can help extend network coverage to areas where the electrical infrastructure cannot reach, or assist during the case of a

natural disaster scenario as the network can work in isolation assuming the presence of the EPC application in the server, where the conventional electricity grid may become unavailable. Also, it avails computation and storage facilities closer to mobile users, even in remote/rural areas. This will overcome the limitations of current Radio Access Networks (RANs), i.e., the lack of computation power and the always-on design approach, as NFV allows the scaling down of some BS functions at low traffic periods or when battery levels are low. However, the integration of MEC and EH base station systems brings about new challenges related to energy consumption, and resource scheduling. Among other things, quantifying the energy consumed by each running VM is a challenge, yet VM power metering is key to power consumption minimization in softwarized clouds [3].

In [4] [5], Energy Savings (ESs) towards BSs have been studied to minimize the BS power consumption by enabling sleep modes at low traffic load periods. For instance, if a BS has not harvested sufficient energy, its transmission power can be tuned to be in proportion to the energy in its local energy storage and, for low traffic load periods, some of the BS functions can be deactivated. ESs within the virtualized computing platform are also of great importance. It is known that the power drawn by the server consists of an *idle* component and a *dynamic* component, which is the power consumed by the physical resources when working on behalf of some VMs. In [6], it is shown that power consumption increases with a growth in the number of virtual entities (e.g., VMs) that are allocated to the physical core, and in [7], it is further experimentally shown that increasing the number of VMs also increases power consumption in virtualized platforms, when taking into account the CPU usage only. From the obtained results [6] [7], the authors observed that the locus of energy consumption for component of Virtualized Network Function (VNF) is the VM instance where the VNF is instantiated/executed. Thus, reducing the number of running VMs at each time instance, i.e., VM soft-scaling, together with BS sleep modes can yield the required energy savings.

Bringing computing and storage services on the BS

for offloading some workloads requires special attention, as resources are limited at the edge. Control-theoretic and Machine Learning (ML) methods for resource management at the edge have been successfully applied to various problems, e.g., task scheduling, bandwidth allocation, network management policies, etc. In [8], the authors presented a generic online control framework for resource management in switching hybrid systems, where the system’s control inputs are finite. The relevant parameters of the operating environment, e.g., workload arrival, are estimated and then used by the system to forecast future behavior over a look-ahead horizon. From this, the controller optimizes the predicted system behavior following the specified Quality of Service (QoS) through the selection of the system control inputs. In [9], a supervisory online control scheme based on Limited Lookahead Controller (LLC) policies is presented. The authors in [10] presents a reinforcement learning-based resource management algorithm to incorporate renewable energy into a MEC platform. At the beginning of the time slot the servers are consolidated, i.e., the number of turned on physical servers are minimized, using the learned optimal policy for dynamic workload offloading and the autoscaling (or right-sizing). Our work differs from [10], as we minimize the number of active VMs instead of server consolidation, and also we use a forecasting method instead of only relying on the available current information for decision making.

Paper contributions: here, we consider the aforementioned scenario, where the BS is equipped with EH hardware and computation capabilities, i.e., a solar panel or wind turbine for EH, an energy storage unit termed Energy Buffer (EB), and a MEC server co-located with the BS. The presence of EB and EH systems promotes energy self-sustainability and network coverage extension. Motivated by the potential of EH and MEC, **1)** we estimate the short-term future traffic load and harvested energy in BSs, by using *Recurrent Neural Networks* (RNNs [11]), specifically a Long Short-Term Memory (LSTM) network, coupled with forecasting knowledge from [12], and **2)** we develop an online algorithm for edge network management based on control theory. The main goal is to enable ES strategies within the remote site through BS sleep modes and VM soft-scaling, following the energy efficiency requirements of a virtualized infrastructure from [13]. The proposed management algorithm is called ENergy Aware and Adaptive Management (ENAAM) and is hosted in the MEC server, i.e., ENAAM Application (App). The ENAAM application considers the future BS loads, onsite green energy in the EB and then provisions edge network resources based on the learned information, i.e., ES decisions are made in a forward-looking fashion.

The proposed optimization strategy reads to a considerable reduction in the energy consumed by edge computing and communication facilities, enabling mobile services to off-grid sites under limited energy budget

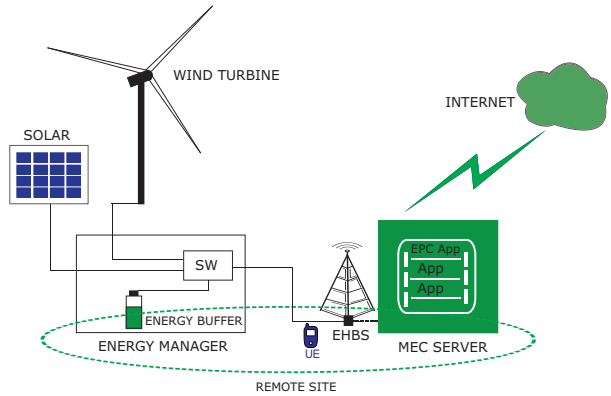


Figure 1: EH BS co-located with a MEC server. The switch (SW) is responsible for selecting the appropriate renewable energy source to power the BS site.

and predicted traffic loads.

The rest of the paper is structured as follows: the system model is presented in Section II. In Section III, we detail the optimization problem and the proposed ENAAM online algorithm. In Section IV, we evaluate our online edge network management algorithm and lastly, we conclude our work in Section V.

II. SYSTEM MODEL

The considered scenario is illustrated in Fig. 1. As a major deployment method of MEC, we consider a setup where a BS is co-located with a virtualized MEC server, forming a communication site *termed* remote site. Both share the available energy stored in the EB. Following the motivation from the introduction, we only consider an *offgrid* BS co-located with the MEC server. The MEC server accounts for M virtual machines as total computation resources, and it is cache-enabled, i.e., some contents can be accumulated locally. Radio network and energy level information is reported periodically to the MEC server through Radio Network Information Services (RNIS) and the Energy Manager (EM), an entity responsible for selecting the appropriate renewable energy source to fulfill the EB depending on the weather, and for monitoring the energy levels in the system. Moreover, we consider a discrete-time model, whereby time is discretized as $t = 1, 2, \dots$, and time slots have a constant duration. For data communication from the remote site to the remote cloud, the system uses a microwave backhaul, as fast roll-out over large distances makes microwave an ideal rural/remote backhaul solution [14].

A. Traffic Load and Power Consumption

Traffic load traces have been obtained using real MN data from the Big Data Challenge organized by Telecom Italia Mobile (TIM) [15]. The open source dataset is a result of users interaction within the TIM MN for the city of Milan during the month of November 2013, whereby each interaction generates a Call Detail Record (CDR) file. The considered TIM dataset refers to standard traffic

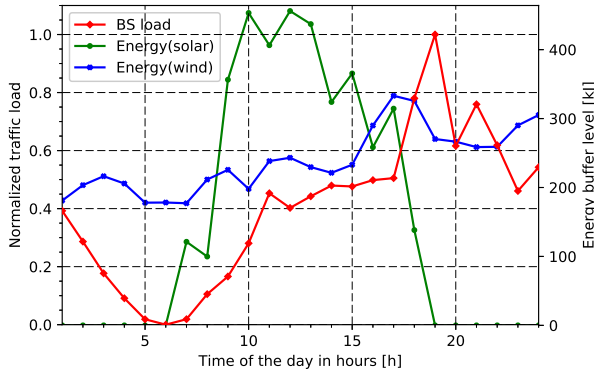


Figure 2: Example traces for harvested solar and wind energy, and normalized traffic load in the BS.

such as SMS, Calls and Internet browsing, and they are not yet a representative of future applications that require processing at the edge. In this paper, according to [16], we assume that 80% of the traffic from this dataset requires processing at the edge, whereas the remaining 20% pertains to standard, delay tolerant, flows. The daily traffic load profile requiring computation at the BS, $L(t)$, see red curve in Fig. 2, is obtained by accounting for 80% of the aggregated CDR data. The normalized BS load at time slot t is approximated as $\varphi(t) = L(t)/L_{\max}$, where L_{\max} represents the maximum load that can be served. Among this load, $\gamma(t) \in [0, 1]$ is processed locally and the rest $\Gamma(t) = \varphi(t) - \gamma(t) \in [0, 1]$ is handled by the remote cloud. Moreover, a low traffic threshold L_{low} is defined to be used in the ENAAM algorithm (see subsection III-B3). Note that $\gamma(t)$ is a decision variable, as we shall see, $\gamma(t)$ is ideally set to 1 for those time slots where the BS has enough energy, i.e., all the delay sensitive traffic is processed at the edge. $\gamma(t)$ will be set to a smaller value otherwise.

The total energy consumption ([kJ]) of the remote site is here obtained as the combination of the energy consumed by the BS and by the co-located MEC server operating at a frequency f ([Hz]), with server maximum utilization factor $\gamma(t)$ in time slot t . The following model is inspired by [17] and [18], by additionally tuning the BS static energy and the server utilization factor, to scale the server dynamic energy consumption in proportion to the expected load to be processed locally,

$$\theta(\zeta, \gamma, t) = \zeta(t)\theta_0 + \theta_{\text{tx}}(t) + \theta_{\text{bh}} + \theta_{\text{mec}}(\gamma, t), \quad (1)$$

where $\zeta(t) \in \{\varepsilon, 1\}$ is the BS switching status indicator (1 for *active mode* and ε for *power saving mode*), θ_0 is a constant value (load independent), representing the operation energy which includes baseband processing, radio frequency power expenditures, etc. The constant $\varepsilon \in (0, 1)$ accounts for the fact that the baseband energy consumption can be scaled down as well whenever there is no or little channel activity, into a power saving mode. $\theta_{\text{tx}}(t)$ represents the total downlink transmission (load dependent) power

from the BS to the served user(s). Since we assume a noise-limited channel and the guarantee of low latency requirements at the edge, to obtain $\theta_{\text{tx}}(t)$ we use the downlink transmission model in [19] (see Eq. (4) in that paper). θ_{bh} is the microwave backhaul transmission energy, which is here assumed to be constant. $\theta_{\text{mec}}(\gamma, t)$ is the computation energy at the server, defined as follows: $\theta_{\text{mec}}(\gamma, t) = \theta_{\text{idle}} + \gamma(t)\theta_{\text{dyn}}(t)$, where $\theta_{\text{idle}}(\cdot)$ is the server load-independent operational component, and $\theta_{\text{dyn}}(\cdot)$ is the maximum energy amount that is consumed by the server when it operates at full power. Although omitted for the sake of notation compactness, θ_{idle} and $\theta_{\text{dyn}}(\cdot)$ depend on the MEC server computation frequency f . Also, $\theta_{\text{dyn}}(\cdot)$ is linearly scaled with respect to the load $\gamma(t)$, assuming that computation resources can be tuned. Finally, the number of virtual machines that shall be active in time slot t to serve the offered load is here obtained as $I(t) = \text{round}(\gamma(t)M)$, where $\text{round}(\cdot)$ rounds the argument to the nearest integer.

B. Energy Patterns and Storage

The energy buffer is characterized by its maximum energy storage capacity β_{\max} . At the *beginning* of each time slot t , the EM provides the energy level report to the MEC server application, thus the EB level $\beta(t)$ is known, enabling the provision of the required computation resources, i.e., VMs. Here, a pull transfer mode (e.g., FTP [20]) is assumed, where the MEC application pulls the energy report from the EM. The amount of harvested energy $H(t)$ in time slot t for the remote site is obtained from open source solar traces from [21] (see green curve in Fig. 2), and also wind traces from [22] (see blue curve in Fig. 2). The datasets are a result of daily environmental records, considering solar panel orientation, measured and forecast wind speed, temperature, wind power, and pressure values. In this paper, $H(t)$ is obtained by first scaling the datasets to fit the EB capacity β_{\max} of 490 kJ, and then selecting the wind energy as a source during the solar energy off-peak periods. Thus, the available EB level $\beta(t+1)$ for the *offgrid* BS in time slot $t+1$ is calculated as follows:

$$\beta(t+1) = \beta(t) + H(t) - \theta(\zeta, \gamma, t) \quad (2)$$

where $\beta(t)$ is the energy level in the battery at the beginning of time slot t and $\theta(\zeta, \gamma, t)$ is the energy that is used during the time slot for computation and communications, see Eq. (1). For decision making in the MEC server, a lower battery threshold is defined, β_{low} , with $0 < \beta_{\text{low}} < \beta_{\max}$, to steer how the energy management algorithm provisions the required edge network resources, see Section III-B.

III. PROBLEM FORMULATION

In this section, we formulate an optimization problem to obtain *energy savings* through short-term traffic load and harvested energy predictions along with energy management procedures. The optimization problem is

defined in section III-A, and the remote site management procedures are presented in Section III-B.

A. Optimization Problem

At the beginning of each time slot t , the MEC server receives the energy level report $\beta(t)$ from the EM. In this paper, we aim at minimizing the overall energy consumption in the remote site over time, i.e., consumption related to the BS and MEC server, by applying BS power saving modes and VM soft-scaling, i.e., tuning the number of active virtual machines. To achieve this, we define two cost functions: F1) $\theta(\zeta, \gamma, t)$, which weighs the energy consumption due to transmission (BS) and computation (MEC server); and F2) a quadratic term $(\varphi(t) - \gamma(t))^2$, which accounts for the QoS cost. In fact, F1 tends to push the system towards energy efficient solutions, i.e., where $\gamma(t) \rightarrow 0$ and $\zeta(t) \rightarrow \varepsilon$. Instead, F2 favors solutions where the load is entirely processed by the local MEC server, i.e., where $\gamma(t) \rightarrow \varphi(t)$. A weight $\alpha \in [0, 1]$, is utilized to balance the two objectives F1 and F2. The corresponding weighted cost function is defined as:

$$J(\zeta, \gamma, t) \triangleq \bar{\alpha}\theta(\zeta(t), \gamma(t), t) + \alpha(\varphi(t) - \gamma(t))^2, \quad (3)$$

where $\bar{\alpha} \triangleq 1 - \alpha$. Hence, over time horizon, $t = 1, \dots, T$, the following optimization problem is defined:

$$\begin{aligned} \mathbf{P1} &: \min_{\zeta, \gamma} \sum_{t=1}^T J(\zeta, \gamma, t) \\ &\text{subject to:} \\ \text{C1} &: 0 < \gamma(t) \leq 1, \quad t = 1, \dots, T \\ \text{C2} &: \zeta(t) \in \{\varepsilon, 1\}, \quad t = 1, \dots, T \\ \text{C3} &: I(t) \geq b, \quad t = 1, \dots, T \\ \text{C4} &: \beta(t) \geq \beta_{\text{low}}, \quad t = 1, \dots, T \end{aligned} \quad (4)$$

where vectors ζ (switching status) and γ (utilization factor) contain the control actions for the considered time horizon $1, 2, \dots, T$, i.e., $\zeta = [\zeta(1), \zeta(2), \dots, \zeta(T)]$ and $\gamma = [\gamma(1), \gamma(2), \dots, \gamma(T)]$. Constraint C1 specifies the server utilization factor bounds, C2 specifies the BS operation status, C3 forces the required number of VMs, $I(t)$, to be always greater than or equal to a minimum number $b \geq 1$: the purpose of this is to be always able to handle mission critical communications. C4 makes sure that the EB level is always above or equal to a preset threshold β_{low} , to guarantee energy self-sustainability over time. To solve P1 in Eq. (4), we leverage the use of LLC [8] [9] and heuristics. Once P1 is solved, the control action to be applied at time t is $\varsigma(t) \triangleq (\zeta(t), \gamma(t))$.

B. Remote Site Management

In this subsection, a traffic load and energy harvesting prediction method, and an online management algorithm are proposed to solve the previously stated problem P1. In subsection III-B1, we discuss the machine learning tool used to predict the short-term future traffic loads

Table I. LSTM Prediction Model Steps

Modeling steps
Step 1: load and normalize the dataset
Step 2: split dataset into training and testing
Step 3: reshape input to be [samples, time steps, features]
Step 4: create and fit the LSTM network
Step 5: make predictions
Step 6: calculate performance measure

and harvested energy, and then in subsection III-B2, we solve P1 by first constructing the state-space behavior of the control system, where online control key concepts are introduced. Finally, the algorithm for managing the remote site is presented in subsection III-B3.

1) *Traffic load and energy prediction*: ML techniques constitute a promising solution for network management and energy savings in cellular networks [11][23]. In this work, we consider a time slot duration of one hour and perform time series prediction, i.e., we obtain the 1 h-ahead estimates of $\hat{L}(t+1)$ and $\hat{H}(t+1)$, by using an LSTM developed in Python using Keras deep learning libraries (Sequential, Dense, LSTM) where the network has a visible layer with 1 input, a hidden layer of 4 LSTM blocks or neurons, and an output layer that makes a single value prediction. This type of recurrent neural network uses back-propagation through time and memory blocks for regression [24]. The dataset is split as 67% for training and 33% for testing. The network is trained using 100 epochs (2,600 individual training trials) with batch size of 1. As for the performance measure of the model, we use the Root Mean Square Error (RMSE). The prediction steps are outlined in Table I, and Fig. 3 show the prediction results that will be discussed in Section IV.

2) *Edge system dynamics*: we denote the system state vector at time t by $x(t) = (I(t), \beta(t))$, which contains the number of active VMs, and the EB level. $\varsigma(t) = (\zeta(t), \gamma(t))$ is the input vector, i.e., the control action that drives the system behavior at time t . The system evolution is described through a discrete-time state-space equation, adopting the LLC principles [8] [9]:

$$x(t+1) = \Phi(x(t), \varsigma(t)), \quad (5)$$

where $\Phi(\cdot)$ is a behavior model that captures the relationship between $(x(t), \varsigma(t))$, and the next state $x(t+1)$. Note that this relationship accounts for 1) the amount of energy drained $\theta(\zeta, \gamma, t)$ and the harvested $H(t)$, which together lead to the next buffer level $\beta(t+1)$ through Eq. (2), and 2) to the traffic load $L(t)$, from which we compute the offered load $\varphi(t)$, that together with the control $\gamma(t)$ leads to $I(t+1)$ (once a control policy is specified). The remote site management ENAAM App, acts as a controller, that finds the best control action vector to the system, iteratively. For each time slot t , the best control action $\varsigma^*(t)$ is the one minimizing the weighted sum $J(\zeta, \gamma, t)$. This control action amounts to setting the BS radio mode $\zeta^*(t)$, i.e., either active or

power saving, and the number of instantiated VMs, $I^*(t)$, which directly follows from $\gamma^*(t)$.

An observation is in order. State $x(t)$ and control $\varsigma(t)$ are respectively measured and applied at the beginning of time slot t , whereas the offered load $L(t)$ and the harvested energy $H(t)$ are accumulated during the time slot and their value becomes known only by the end of it. This means that, being at the beginning of time slot t , the system state at the next time slot $t + 1$ can only be estimated, which we formally write as:

$$\hat{x}(t+1) = \Phi(x(t), \varsigma(t)). \quad (6)$$

Controller decision-making: the controller is obtained by estimating the relevant parameters of the operating environment, that in our case are the BS load $\hat{L}(t)$ and the harvested energy $\hat{H}(t)$, and subsequently using them to forecast the future system behavior through Eq. (6) over a look-ahead time horizon of T time slots. The control actions are picked by minimizing $J(\zeta, \gamma, t)$, see Eq. (3). At the beginning of each time slot t the following process is iterated:

- Future system states, $\hat{x}(t+k)$, for a prediction horizon of $k = 1, \dots, T$ steps are estimated using Eq. (3). These predictions depend on past inputs and outputs up to time t , on the estimated load $\hat{L}(\cdot)$ and energy harvesting $\hat{H}(\cdot)$ processes, and on the control $\varsigma(t+k)$, with $k = 0, \dots, T-1$.
- The sequence of controls $\{\varsigma(t+k)\}_{k=0}^{T-1}$ is obtained for each step of the prediction horizon by optimizing the weighted cost function $J(\cdot)$.
- The control $\varsigma^*(t)$ corresponding to the first control action in the sequence with the minimum total cost is the applied control for time t and the other controls $\varsigma^*(t+k)$ with $k = 1, \dots, T-1$ are discarded.
- At the beginning of the next time slot $t+1$, the system state $x(t+1)$ becomes known and the previous steps are repeated.

3) *The ENAAM algorithm:* Let t be the current time. $\hat{L}(t+k-1)$ is the forecast load in slot $t+k-1$, with $k = 1, \dots, T$, i.e., over the prediction horizon. For the control to be feasible, we have $\hat{\varphi}(t+k-1) = \hat{L}(t+k-1)/L_{\max}$ and $\underline{\gamma} \leq \gamma \leq \hat{\varphi}(t+k-1)$, where $\underline{\gamma}$ is the smallest γ such that $\text{round}(\underline{\gamma}M) = b$. For the buffer state, we heuristically set $\zeta(t+k-1) = \varepsilon$ if $\beta(t+k-1) < \beta_{\text{low}}$ or $L(t+k-1) < L_{\text{low}}$, and $\zeta(t+k-1) = 1$ otherwise (β_{low} and L_{low} are preset thresholds). For slot $t+k-1$, the feasibility set $\mathcal{A}(t+k-1)$ contains the control pairs (ζ, γ) that obey these relations.

The algorithm is specified in Alg. 1 as it uses the technique in [8]: the search starts (line 01) from the system state at time t , $x(t)$, and continues in a breadth-first fashion, building a tree of all possible future states up to the prediction depth T . A cost is initialized to zero (line 01) and is accumulated as the algorithm travels through the tree (line 06), accounting for predictions,

Algorithm 1: ENAAM

Input: $x(t)$ (current state)
Output: $\varsigma^*(t) = (\zeta^*(t), \gamma^*(t))$
01: Initialization of variables
 $\mathcal{S}(t) = \{x(t)\}$, $\text{Cost}(x(t)) = 0$
02: **for** $k = 1, \dots, T$ **do**
- forecast the load $\hat{L}(t+k-1)$
- forecast the harvested energy $\hat{H}(t+k-1)$
- $\mathcal{S}(t+k) = \emptyset$
03: **for all** $x \in \mathcal{S}(t+k-1)$ **do**
04: **for all** $\varsigma = (\zeta, \gamma) \in \mathcal{A}(t+k-1)$ **do**
05: $\hat{x}(t+k) = \Phi(x(t+k-1), \varsigma)$
06: $\text{Cost}(\hat{x}(t+k)) = J(\zeta, \gamma, t+k-1)$
+ $\text{Cost}(x(t+k-1), \varsigma)$
07: $\mathcal{S}(t+k) = \mathcal{S}(t+k) \cup \{\hat{x}(t+k)\}$
end for
end for
end for
08: **Find** $\hat{x}_{\min} = \text{argmin}_{\hat{x} \in \mathcal{S}(t+T)} \text{Cost}(\hat{x})$
09: $\varsigma^*(t) :=$ control leading from $x(t)$ to \hat{x}_{\min}
10: **Return** $\varsigma^*(t)$

past outputs and controls. The set of states reached at every prediction depth $t+k$ is referred to as $\mathcal{S}(t+k)$. For every prediction depth $t+k$, the search continues from the set of states $\mathcal{S}(t+k-1)$ reached at the previous step $t+k-1$ (line 03), exploring all feasible controls (line 04), obtaining the next system state from Eq. (6) (line 05), updating the accumulated cost as the result of the previous accumulated cost, plus the cost associated with the current step (line 06), and updating the set of states reached at step $t+k$ (line 07). When the exploration finishes, the action at time t that leads to the best final accumulated cost, at time $t+T$, is selected as the optimal control $\varsigma^*(t)$ (lines 08, 09, 10). Finally, for line 04, we note that γ belongs to the continuous set $[\underline{\gamma}, \hat{\varphi}(t+k-1)]$. To implement this search, we quantized this interval into a number of equally spaced points, obtaining a search over a finite set of controls.

IV. PERFORMANCE EVALUATION

In this section we show some selected numerical results for the scenario of Section II. The parameters that were used for the simulations are listed in Table II. **Simulation Setup:** we consider one offgrid BS co-located with a MEC server within a coverage area of 40 m. In addition, we use a virtualized server with specifications from [25] for a VMware ESXi 5.1-ProLiant DL380 Gen8 that operates at $f = 1,600$ MHz. Our time slot duration is set to 1 h and the time horizon to $T = 2$. For our simulations, Python is used as the programming language.

Numerical Results: some example prediction results are shown in Fig. 3 for the traffic load, reaching an RMSE performance of 0.42 MB. Quite good accuracies

Table II. System Parameters.

Parameter	Value
Low traffic threshold, L_{low}	4 MB
Maximum load, L_{max}	15 MB
Operating power, θ_0	10.6 W
Microwave backhaul power, θ_{bh}	50 W
Maximum number of VMs, M	27
Minimum number of VMs, b	3
Idle power, θ_{idle}	30 W
Dynamic maximum power, $\theta_{dyn}(t)$	472.3 W
Energy storage capacity, β_{max}	490 kJ
Lower energy threshold, β_{low}	30% of β_{max}
Maximum number of served users	50

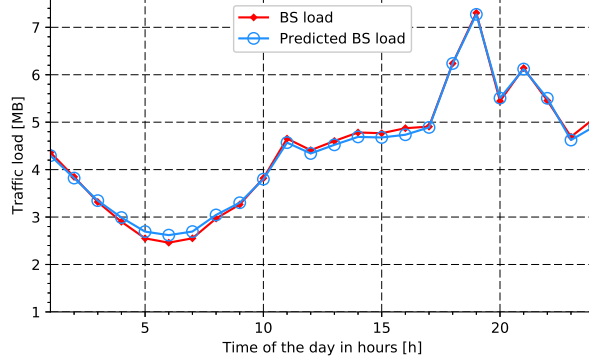


Figure 3: One-step ahead predicted BS load (LSTM).

are also obtained for the prediction of the harvested energy (RMSE of 0.38 kJ over a range of about 450 kJ). The measured accuracy is deemed good enough for the proposed optimization.

Figs. 4 and 5 show the energy savings achieved over time for $\alpha = 0$ and $\alpha = 0.5$ respectively, when on-demand and energy-aware edge resource provisioning is enabled (i.e., BS sleep modes and VM soft-scaling), in comparison with the case where they are not applied. Our remote site management algorithm (ENAAM) is benchmarked with another one that heuristically selects the amount of traffic that is to be processed locally, $\gamma(t)$, depending on the expected load behavior. It is named Dynamic and Energy-Traffic-Aware algorithm with Random behavior (DETA-R). Both ENAAM and DETA-R are aware of the predictions in the future time slots, see Section III-B1, however, DETA-R provisions edge resources using a heuristic scheme. DETA-R heuristic works as follows: if the expected load difference is $\hat{L}(t+1) - \hat{L}(t) > 0$, then $\gamma(t)$ in the current time slot t is randomly selected in the range $[0.6, 1]$, otherwise, it is picked evenly at random in the range $(0, 0.6)$.

When $\alpha = 0$, Fig. 4 shows energy savings of 66% on average when ENAAM scheme is applied, while DETA-R achieves 32%, where these savings are with respect to the case where *no energy management* is performed, i.e., the network is dimensioned for maximum expected capacity (maximum value of $\theta(\zeta, \gamma, t)$, $M = 27$ VMs, $\forall t$). A peak can be observed in the performance of DETA-R between 4 h and 7 h where it approaches close

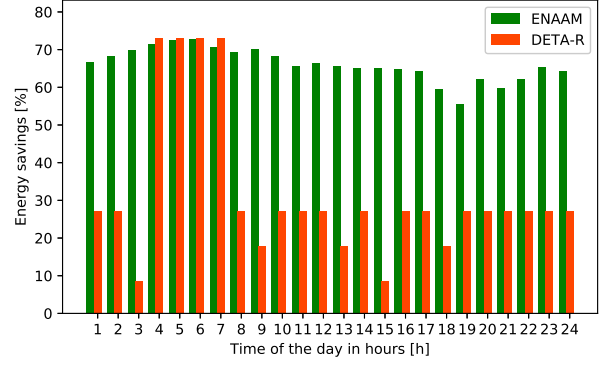


Figure 4: Hourly energy savings for $\alpha = 0$.

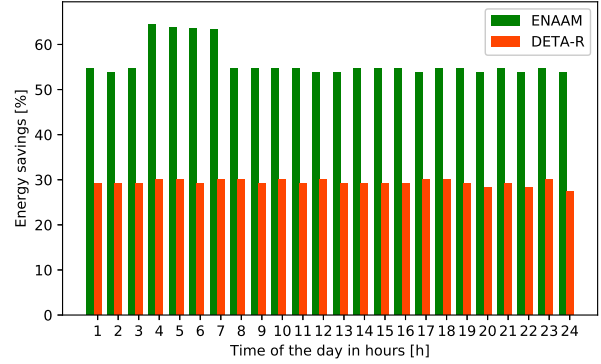


Figure 5: Hourly energy savings for $\alpha = 0.5$.

to ENAAM. This is due to a decrease in the expected traffic load, which translates into low server utilization ($0 \leq \gamma \leq 0.5$) and high energy savings. Note that $\alpha = 0$ leads to the highest energy savings, where the BS radio frontend is moved as often as possible into sleep mode and the minimum number b of VMs is active in all time slots. While this may be meaningful as an energy consumption lower-bound, a more interesting choice is provided by $\alpha > 0$, where the local processing cost is also taken into account.

In Fig. 5 ($\alpha = 0.5$), the ENAAM scheme achieves ESs of about 56% and DETA-R of 29% on average. As expected, this shows a reduction in energy savings compared to when $\alpha = 0$. This is due to the balance between the emphasis on energy savings and QoS, i.e., locally computed tasks, within the remote site. The evolution of ESs with respect to α is presented in Fig. 6. As expected, a drop in energy savings is observed when QoS is prioritized, i.e., $\alpha \rightarrow 1$, as in this case the BS energy consumption is no longer considered.

Finally, Fig. 7 shows the MEC server utilization over time, i.e., the selected control $\gamma(t)$. For $\alpha = 0.5$, the server utilization is about 76% for ENAAM and 95% for DETA-R on average. A low server utilization can be observed in the performance of ENAAM between 4 h and 7 h due to an expected low traffic load in the system. This indicates that ENAAM has load adaptation capabil-

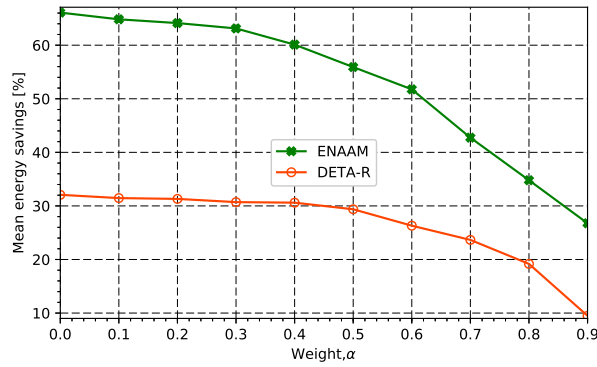


Figure 6: Energy savings vs the optimization weight α .

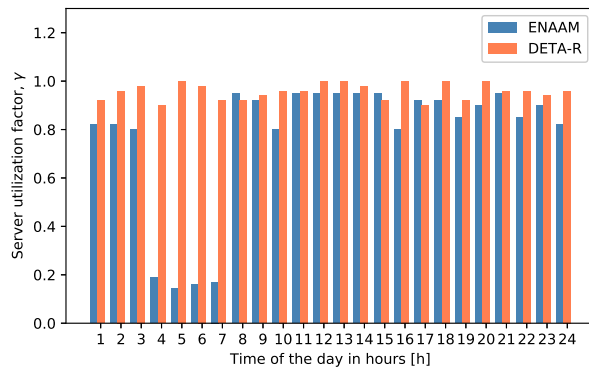


Figure 7: MEC server utilization ($\alpha = 0.5$).

ities, which are much desirable and lead to substantial energy savings (see again Fig. 5 between 4 h and 7 h).

V. CONCLUSIONS

In this paper, we have envisioned a renewable-powered remote site for extending network coverage and promote energy self-sustainability within mobile networks. The BS at the remote site is endowed with computation capabilities for guaranteeing low latency to mobile users, offloading their workloads. The combination of the energy saving methods, namely, BS sleep modes and VM soft-scaling, for the remote site helps to reduce its energy consumption. An edge energy management algorithm based on forecasting, control theory and heuristics, is proposed with the objective of saving energy within the remote base station, possibly making the BS system self-sustainable. Numerical results, obtained with real-world energy and traffic traces, demonstrate that the proposed algorithm achieves energy savings between 56% and 66% on average, with respect to the case where no energy management techniques are applied, and to hold the server utilization between 30% and 96% over time, with an average of 75%.

VI. ACKNOWLEDGEMENTS

This work has received funding from the European Union's Horizon 2020 research and innovation pro-

gramme under the Marie Skłodowska-Curie grant agreement No. 675891 (SCAVENGE).

REFERENCES

- [1] M. Patel, Y. Hu, P. Hédé, J. Joubert, C. Thornton, B. Naughton, J. R. Ramos, C. Chan, V. Young, S. J. Tan, D. Lynch, N. Sprecher, T. Musiol, C. Manzanara, U. Rauschenbach, S. Abeta, L. Chen, K. Shimizu, A. Neal, P. Cosimini, A. Pollard, and G. Klas, "Mobile edge computing introductory technical white paper," ETSI, Sophia-Antipolis, France, Tech. Rep., Sep. 2014.
- [2] D. Zordan, M. Miozzo, P. Dini, and M. Rossi, "When telecommunications networks meet energy grids: cellular networks with energy harvesting and trading capabilities," *IEEE Communications Magazine*, vol. 53, no. 6, pp. 117–123, 2015.
- [3] C. Gu, H. Huang, and X. Jia, "Power Metering for Virtual Machine in Cloud Computing-Challenges and Opportunities," *IEEE Access*, vol. 2, pp. 1106–1116, 2014.
- [4] E. Oh, B. Krishnamachari, X. Liu, and Z. Niu, "Toward dynamic energy-efficient operation of cellular network infrastructure," *IEEE Communications Magazine*, vol. 49, no. 6, 2011.
- [5] J. Erman and K. K. Ramakrishnan, "Understanding the super-sized traffic of the super bowl," in *Proceedings of the 2013 conference on Internet measurement conference*, Barcelona, Spain, Oct. 2013.
- [6] R. Morabito, "Power Consumption of Virtualization Technologies: An Empirical Investigation," in *IEEE International Conference on Utility and Cloud Computing (UCC)*, Limassol, Cyprus, Dec. 2015.
- [7] Y. Jin, Y. Wen, and Q. Chen, "Energy efficiency and server virtualization in data centers: An empirical investigation," in *IEEE Conference on Computer Communications Workshops (INFOCOM Workshops)*, Orlando, USA, Mar. 2012.
- [8] S. Abdelwahed, N. Kandasamy, and S. Neema, "Online control for self-management in computing systems," in *IEEE Real-Time and Embedded Technology and Applications Symposium (RTAS)*, Toronto, Ontario, Canada, May 2004.
- [9] S.-L. Chung, S. Lafortune, and F. Lin, "Limited lookahead policies in supervisory control of discrete event systems," *IEEE Transactions on Automatic Control*, vol. 37, pp. 1921–1935, 1992.
- [10] J. Xu and S. Ren, "Online Learning for Offloading and Autoscaling in Renewable-Powered Mobile Edge Computing," in *IEEE Global Communications Conference (GLOBECOM)*, Washington, USA, Dec. 2016.
- [11] Mingzhe Chen and Ursula Challita and Walid Saad and Changchuan Yin and Mérouane Debbah, "Machine Learning for Wireless Networks with Artificial Intelligence: A Tutorial on Neural Networks," *IEEE Wireless Communications*, Oct 2017. [Online]. Available: <https://arxiv.org/abs/1710.02913>
- [12] R. Hyndman and G. Athanasopoulos, *Forecasting: principles and practice*. OTexts: Melbourne, Australia, 2013.
- [13] "Network Functions Virtualisation (NFV): Hypervisor Domain," ETSI, Sophia-Antipolis, France, Tech. Rep., Jan. 2015.
- [14] "Ericsson Microwave Outlook: Trends and Needs in the microwave Industry," Ericsson, Sweden, Tech. Rep., Oct. 2016.
- [15] "Open Big Data Challenge," 2015. [Online]. Available: <https://dandelion.eu/datamine/open-big-data>
- [16] F. B. Abdesslem and A. Lindgren, "Large scale characterisation of YouTube requests in a cellular network," in *Proceeding of IEEE International Symposium on a World of Wireless, Mobile and Multimedia Networks*, Sydney, NSW, Australia, Jun 2014.
- [17] P. S. Yu, J. Lee, T. Q. S. Quek, and Y. W. P. Hong, "Traffic Offloading in Heterogeneous Networks With Energy Harvesting Personal Cells-Network Throughput and Energy Efficiency," *IEEE Transactions on Wireless Communications*, vol. 15, no. 2, pp. 1146–1161, 2016.
- [18] L. Haikun, X. Cheng-Zhong, J. Hai, G. Jiayu, and L. Xiaofei, "Performance and Energy Modeling for Live Migration of Virtual Machines," in *Proceedings of the 20th International Symposium on High Performance Distributed Computing*, San Jose, California, USA, June 2011.
- [19] L. Chen, S. Zhou, and J. Xu, "Energy Efficient Mobile Edge Computing in Dense Cellular Networks," in *IEEE International Conference on Communications (ICC)*, Paris, France, May 2017.
- [20] "3GPP TS 32.2.297, Charging Data Record (CDR) file format and transfer," ETSI, Sophia-Antipolis, France, Tech. Rep., Aug 2016.
- [21] "Solar Radiation Measurement Data." [Online]. Available: <https://energydata.info/dataset/armenia-solar-radiation-measurement-data-2017>
- [22] "Wind-power Generation Data." [Online]. Available: <http://www.elia.be/en/grid-data/power-generation/wind-power>
- [23] C. Jiang and H. Zhang and Y. Ren and Z. Han and K. C. Chen and L. Hanzo, "Machine Learning Paradigms for Next-Generation Wireless Networks," *IEEE Wireless Communications*, vol. 24, no. 2, pp. 98–105, Apr 2017.
- [24] I. Goodfellow, Y. Bengio, and A. Courville, *Deep Learning*. MIT Press, 2016.
- [25] "Standard Performance Evaluation Corporation," SPEC, Gainesville, Virginia, USA, Tech. Rep., May 2013. [Online]. Available: https://www.spec.org/virt_sc2013/results/specvirt_sc2013_perf.html